CENTRE DE RECHERCHE
SUR LES STRATÉGIES ÉCONOMIQUES

Carbon Pricing, Behavioral Nudges, and Network Effects in Carpooling: A Micro-founded Framework

Moustapha Mounmemi, Vincent Bertrand, Philippe Canalda

June 2026

Working paper No. 2026 – 02

CRESE
30, avenue de l'Observatoire
25009 Besançon
France
http://crese.univ-fcomte.fr/

The views expressed are those of the authors and do not necessarily reflect those of CRESE.

UNIVERSITÉ MARIE & LOUIS PASTEUR

Carbon Pricing, Behavioral Nudges, and Network Effects in Carpooling: A Micro-founded Framework

Moustapha MOUNMEMI[1]
Université Marie et Louis Pasteur, CRESE (UR 3190), F-25000 Besançon, France
Université Marie et Louis Pasteur, Chaire REEL.i, Réseau EDEN.i

Vincent BERTRAND
Université Marie et Louis Pasteur, CRESE (UR 3190), F-25000 Besançon, France
Université Marie et Louis Pasteur, Chaire REEL.i, Réseau EDEN.i

Philippe CANALDA
Université Marie et Louis Pasteur, CNRS, institut FEMTO-ST (UMR 6174), F-25000 Besançon, France

Abstract

Decarbonizing transport requires scalable alternatives to private vehicles, yet carpooling adoption remains limited due to coordination failures and weak network density. This paper develops a micro-founded framework of multimodal carpooling adoption under carbon pricing, behavioral nudges, and endogenous network effects. Agents choose between private transport and platform-based carpooling based on generalized costs and a participation-dependent matching probability. This generates nonlinear adoption dynamics, multiple equilibria, and tipping points driven by network externalities and matching efficiency. The model is calibrated using French mobility evidence and simulation-based methods. Results show that carbon pricing increases adoption but is constrained by coordination thresholds. Behavioral nudges significantly reduce these thresholds and amplify pricing effects. Platform efficiency critically determines whether the system converges to high or low adoption equilibria. Mu-CAR digital platform, currently under deployment, will provide future high-frequency mobility data enabling structural estimation and empirical validation. Overall, the framework highlights strong policy complementarities and network effects.

Keywords. Carbon Pricing, Behavioral Nudges, Network Effects, Carpooling, Matching friction, Micro-founded Framework

[1] moustapha.mounmemi@univ-fcomte.fr

1. Introduction

The transport sector is one of the largest contributors to global greenhouse gas emissions, largely driven by intensive private vehicle use in urban areas across Europe (European Commission, 2023). In this context, shared mobility solutions such as carpooling and ride-sharing have emerged as promising instruments to reduce congestion, energy consumption, and CO_2 emissions. However, despite their potential, adoption rates remain persistently low. The existing literature documents that carpooling participation is still marginal (Correia & Viegas, 2011; Gheorghiu & Delhomme, 2018; Monchambert, 2020), even in relatively advanced contexts such as France, where carpooling represents only about 0.5% of total kilometers traveled annually (Astier et al., 2023; Laroche, 2022). Yet, meeting national decarbonization objectives requires a rapid scaling-up of these practices. The French government has therefore announced the goal of tripling carpooling trips by 2030, increasing from around 900,000 trips in 2022 to 3 million by 2027 (Laroche & Schemeleva, 2026). Understanding the mechanisms that drive carpooling adoption is thus essential for designing effective mobility and climate policies.

Several factors may explain the limited diffusion of carpooling. First, economic incentives—such as subsidies, pricing schemes, or carbon taxes—can affect individuals' travel choices by altering relative costs (Shaheen & Cohen, 2013; Laroche & Schemeleva, 2026). Second, behavioral interventions (nudges) may influence decisions by changing perceptions, habits, or social norms (Salihou et al., 2026). Third, adoption may depend on network effects, since the attractiveness of carpooling increases with the number of participants, generating coordination problems and potentially multiple equilibria (Katz & Shapiro, 1985; Rochet & Tirole, 2003). While each mechanism has been studied separately, their joint interactions remain insufficiently understood. In particular, existing work rarely provides an integrated framework combining economic incentives, behavioral nudges, and network-driven adoption dynamics under platform frictions and matching uncertainty.

This paper addresses this gap by developing a unified micro-founded framework for multimodal carpooling adoption that explicitly integrates carbon pricing, behavioral nudges, and network effects. Individuals are modeled as heterogeneous agents who choose among transport modes based on a random utility approach (McFadden, 1974; Totouom, 2024). In this setting, carpooling adoption depends not only on individual preferences and policy incentives, but also on the endogenous probability of being matched with other users through the platform. This matching uncertainty plays a central role: the perceived utility of carpooling depends on platform efficiency, which itself increases with participation. As a result, adoption dynamics can exhibit nonlinearities, multiple equilibria, and tipping points (Simon & Blume, 1994; Otto et al., 2020), implying that marginal interventions may fail unless policies are sufficiently strong and coordinated.

The paper makes three main contributions. First, it proposes a structural framework that jointly models carbon pricing, behavioral nudges, and network effects, allowing for nonlinear interactions and policy complementarities in multimodal transport choices. Second, it introduces matching uncertainty as an endogenous driver of carpooling behavior, capturing platform frictions and feedback loops between participation and service quality. Third, it provides policy-relevant insights by identifying conditions under which coordinated interventions can trigger large-scale adoption. Our results suggest that adoption tipping dynamics are primarily driven by matching efficiency and network effects, while behavioral nudges mainly operate by shifting coordination thresholds and amplifying the effectiveness of carbon pricing.

To operationalize the model and study equilibrium adoption patterns, we implement large-scale agent-based simulations (Epstein, 2012). This approach allows us to approximate adoption equilibria, detect tipping points, and explore the nonlinear responses of adoption to combined policy instruments. The framework will be embedded within the Mu-CAR project, a real-world digital platform[2] designed to test policy interventions in mobility behavior (Gaspoz et Canalda, 2024 ; Joliot et al., 2025). The platform is developed in-house by researchers in computer science within our consortium, with the objective of combining algorithmic innovation (matching, AI) and behavioral experimentation. By linking theoretical modeling with empirical opportunities, our approach generates testable predictions that can be validated using real-time experimental data collected through the Mu-CAR platform. Overall, this framework provides

[2] https://projects.femto-st.fr/Mu-CAR/fr/actualites/premieres-nouvelles-du-projet-mu-car-2024-2027

policymakers with an evidence-based tool to design effective interventions aimed at accelerating the diffusion of low-carbon shared mobility. Its flexibility allows direct application to real-world platforms, supporting the evaluation of carbon pricing, behavioral nudges, and network design in shaping sustainable travel behavior, and ultimately contributing to the decarbonization of urban and rural mobility.

2. Context, Data, and Experimental Platform: The Mu-CAR Project

Mu-CAR (Multimodal Car-pooling in a Global and Public Intelligent Transport System) is a project funded by the Bourgogne–Franche-Comté Region in France. Its objective is to design and deploy an innovative digital platform for multimodal carpooling, relying on advanced computational tools (matching algorithms, artificial intelligence, and deep learning) to improve real-time coordination between ride offers and ride requests. A central aim of the project is to facilitate modal shift toward public transport networks, particularly for users living in rural and peri-urban areas where accessibility to public transport remains limited.

2.1. Policy and Mobility Context

The Mu-CAR project emerges in a context where decarbonizing transport requires scalable alternatives to single-occupancy vehicle (SOV) commuting. While carpooling and shared mobility solutions have expanded in recent years, adoption remains limited, especially outside dense urban areas. In such environments, carpooling is constrained by low network density, uncertainty in matching opportunities, and persistent coordination failures. These frictions highlight the need for integrated policy tools combining monetary incentives, behavioral interventions, and improvements in platform design and efficiency.

Mu-CAR is explicitly designed to address these constraints by providing a public-oriented intelligent transport system (ITS) infrastructure that supports multimodal mobility and enhances the reliability of shared rides through algorithmic optimization and real-time coordination.

2.2. Digital Platform and Experimental Design

The core innovation of Mu-CAR lies in the deployment of a digital application targeted at real-world users. The platform is conceived as a large-scale living laboratory that enables the implementation of alternative policy configurations and the observation of behavioral responses in actual mobility conditions. It will provide a unique experimental environment to study the

determinants of carpooling adoption and to analyze how individuals adjust their travel behavior in response to economic and behavioral incentives. The platform supports the implementation of both monetary and non-monetary interventions. Monetary incentives take the form of carbon-based rewards, where users are compensated proportionally to the emissions reductions generated through shared trips, based on a reference carbon price. Non-monetary interventions include behavioral nudges, such as informational messages, social norm feedback, default options, and salience-enhancing mechanisms designed to influence perceptions, habits, and decision-making processes.

In addition, the platform allows experimentation with system design and operational features, including improvements in matching algorithms and real-time coordination tools that affect service reliability and waiting times. This design enables the analysis of not only the direct effects of policy instruments on adoption, but also their interaction with endogenous network dynamics, which are central to understanding diffusion processes and potential coordination failures in shared mobility systems.

2.3. Data Collection and Empirical Opportunities

A key contribution of Mu-CAR will be its ability to generate high-frequency, fine-grained mobility data that are typically unavailable in standard survey-based approaches. Operating as a real-world digital platform, Mu-CAR will enable continuous data collection on user behavior and system performance. In particular, the platform will record:

- individual mobility choices and modal combinations,
- detailed trip characteristics (origin–destination pairs, departure times, travel distances),
- matching outcomes (successful vs unsuccessful matches),
- waiting times and coordination frictions,
- user participation dynamics over time, including entry, exit, and repeated adoption behavior,
- heterogeneous responses to monetary incentives and behavioral messages.

This rich data environment will provide a unique empirical basis for analyzing both micro-level decision processes and macro-level participation dynamics, including the emergence of nonlinear adoption patterns and potential tipping points in carpooling diffusion. Importantly, it will also enable the empirical estimation of key structural components of the model developed in this paper, such as the matching probability function and the strength of network externalities.

2.4. Link with the Structural Framework

The theoretical framework developed in this paper is explicitly designed to be structurally compatible with the Mu-CAR platform. It integrates three key mechanisms: (i) monetary incentives based on carbon pricing, (ii) behavioral nudges affecting perceived utility and decision heuristics, and (iii) endogenous network effects driven by aggregate participation and matching success. Although Mu-CAR implements carbon incentives through a carbon reward scheme (a subsidy proportional to avoided emissions), our model represents this mechanism through an equivalent carbon price signal. In our framework, rewarding low-carbon trips is analytically equivalent to increasing the generalized cost of carbon-intensive travel, since both shift relative costs and thus affect modal choice. We abstract from the public budget constraint and focus on behavioral and equilibrium adoption effects.

Crucially, the Mu-CAR platform is not merely a contextual illustration but constitutes the future empirical backbone of the model. It will provide a unique environment for the structural estimation, calibration, and causal validation of the mechanisms embedded in the framework. In particular, the platform will generate exogenous and quasi-experimental[3] variation in policy parameters, enabling the identification of heterogeneous behavioral responses and nonlinear treatment effects. More broadly, the model is designed as a structural framework that is empirically identifiable and directly testable using real-world mobility data. In this sense, Mu-CAR transforms the model from a purely theoretical construct into a data-driven policy laboratory, where structural predictions can be confronted with observed behavior in real time.

2.5. Policy Relevance and Operational Contribution

By combining a real-world ITS deployment with a micro-founded structural model, Mu-CAR provides a concrete framework for evidence-based transport policy design. The project aims to deliver actionable insights for public decision-makers on how to scale multimodal carpooling through coordinated interventions, particularly in low-density territories where coordination failures are most severe.

Ultimately, Mu-CAR contributes to the development of an integrated low-carbon mobility system in which private vehicles, carpooling, and public transport are jointly optimized. The platform facilitates knowledge transfer to local authorities and industry stakeholders, offering

[3] Quasi-experimental variation, meaning variation arising from naturally occurring changes in platform conditions (e.g., phased implementation across areas, time-specific adjustments in incentives, or capacity constraints) that are not driven by users' unobserved preferences.

operational tools to address energy poverty, territorial fragmentation, and decarbonization objectives.

3. Literature Review

The adoption of shared and sustainable transport modes is shaped by a complex interplay of economic incentives, psychological factors, and network effects. Understanding these drivers is critical for designing policies that effectively reduce reliance on single-occupancy vehicles (SOVs) and promote low-carbon mobility.

3.1. Economics incentives and Carpooling Adoption

Financial incentives are the most effective policy lever to promote carpooling and reduce SOV dependency, despite structural and behavioral barriers such as schedule constraints, route mismatches, and perceived inconvenience (Baldassare et al., 1998; Ungemah et al., 2007; Neoh et al., 2017; Standing et al., 2019; Tafreshian & Masoud, 2020). Economic instruments—whether compensating for lost comfort or flexibility—have consistently increased participation in shared mobility schemes (Konishi & Mun, 2010; Julagasigorn et al., 2021; Salihou et al., 2026; Wang & Monchambert, 2026).

These measures typically take the form of taxes—fuel levies, vehicle excise duties, parking fees, road pricing—or public transport subsidies. Direct CO_2-targeted policies are particularly effective: a €0.016 per liter fuel tax reduced SOV use by 1.1%, increased public transport ridership by 14.2%, and walking by 1.3%. In comparison, a 50% increase in parking fees reduced SOV use by 0.8%, raised public transport by 4.5%, and walking by 1.7%, while a €1.2 daily road pricing charge decreased SOV use by 0.7% and increased public transport by 9.2% (Hammadou & Papaix, 2015; Pavon & Rizzi, 2019). Subsidies complement these instruments by encouraging modal shifts among non-car-owning commuters in areas with good transit access (Rotaris & Danielis, 2014; De Witte et al., 2013; Bueno et al., 2017). Comparative evidence highlights that direct pricing measures consistently outperform subsidies, particularly for employees and managers, while subsidies remain effective in specific contexts where transit accessibility is high.

3.2. Psychological Factors and Persuasive Interventions

Transport mode choice is strongly influenced by psychological determinants, including subjective norms, individual perceptions, habits, and personal attitudes (Shang-Yu Chen, 2016;

Lind et al., 2015; De Vos et al., 2020). Subjective norms—perceived social pressures—are especially influential in urban areas, motivating both users and non-users of active modes such as cycling. However, individual attitudes emerge as the most robust predictor of sustainable mode adoption, shaping public transport use among adults and travel choices for children based on well-being during trips (De Vos et al., 2020). For rural populations, intentions to adopt public transport improve when accessibility is enhanced, underscoring the interaction between personal attitudes and infrastructure availability.

Persuasive technologies provide a complementary pathway to reinforce adoption. Feedback and self-assessment mechanisms boost cycling uptake among existing users (Piwek et al., 2015), while tailored messaging promotes walking, with age-specific motivators: health benefits for older adults, environmental awareness for younger individuals (Pangbourne et al., 2020; Bucher et al., 2019; Tsirimpa et al., 2019). Personality traits and argumentative messaging further increase intervention effectiveness, illustrating the potential of behaviorally informed, targeted strategies to enhance sustainable travel.

3.3. Network Effects and carpooling adoption

Beyond economic and psychological drivers, network effects play a pivotal role in shaping carpooling adoption. Individuals are more likely to participate as peer adoption increases, generating positive feedback loops and potential tipping points (Katz & Shapiro, 1985; Rochet & Tirole, 2003). High participation improves matching probabilities, reduces travel uncertainty, and reinforces perceived social norms, strengthening behavioral shifts toward sustainable modes.

Empirical evidence shows that network externalities amplify the effects of economic and behavioral interventions. Early-stage adoption incentives can trigger cascading effects, where modest initial uptake leads to broader participation (Correia & Viegas, 2011; Monchambert, 2020). Conversely, low participation may limit the effectiveness of both subsidies and direct pricing. Children, commuters, and urban residents are particularly sensitive to network effects, as they are more sensitive on peer participation that influences perceived convenience, safety, and social acceptability. Integrating network considerations—through incentives for early adopters or visibility of active users—can accelerate adoption and overcome coordination failures in urban and suburban contexts.

4. Micro-Founded Model

4.1. Population and Heterogeneity

We consider a continuum of individuals indexed by $i \in [0,1]$. Each individual chooses between two transport modes: T (individual private transport) and C (multimodal carpooling). Individuals are heterogeneous in their responsiveness to economic incentives, behavioral interventions, and social motivations. Each agent is characterized by the vector :

$$\boldsymbol{\theta_i = (\alpha_i, \beta_i)} \quad \textbf{(1)}$$

Where, α_i measures sensitivity to carbon-based monetary incentives,β_i captures responsiveness to behavioral nudges. We assume that the vector θ_i is drawn from a joint distribution $F(\theta)$ with compact set and strictly positive density.

4.2. Utility with endogenous matching probability

We rely on the random utility framework developed by McFadden (1974) to model individuals' transport choices. This framework has recently been implemented by Mounmemi and Kouandou (2026) in the context of the energy transition. It allows us to represent heterogeneous preferences and stochastic adoption decisions, where each individual chooses the alternative that maximizes their perceived utility. We consider two transport alternatives: private transport T(solo driving) and multimodal carpooling C. Multimodal carpooling is interpreted as a mobility bundle combining a shared car segment with access/egress legs (walking, public transport) and transfer frictions. These multimodal components are summarized in a generalized cost term C_i^C, which includes travel time, monetary expenses, coordination costs, and transfer penalties.

In reality, the adoption of multimodal carpooling is influenced not only by economic incentives and behavioral interventions but also by the uncertainty associated with finding a suitable carpooling match. So, a key feature of multimodal carpooling is that its benefits are realized only if an individual successfully finds a match on the platform. We capture this matching friction by introducing a participation-dependent probability of successful matching $q(P) \in [0,1]$, where P denotes the aggregate participation rate. We assume:

$$\boldsymbol{q(P) = 1 - \exp(-\kappa P)}, \quad \textbf{(2)}$$

where $\kappa > 0$ measures platform efficiency. A low value of κ corresponds to severe matching frictions (low platform efficiency), whereas a high κ implies a more efficient platform with higher match reliability. This functional form implies that when participation is low, matching success is unlikely, while for large P, the probability of finding a match approaches one. The utility from private transport is:

$$\boldsymbol{U_i^T = Y_i - C_i^T.} \quad \textbf{(3)}$$

The expected utility from multimodal carpooling is:

$$\boldsymbol{U_i^C = Y_i - C_i^C + q(P)(\alpha_i p_c E + \beta_i n + \eta P),} \quad \textbf{(4)}$$

where p_c is the carbon price[4] (implicit carbon price), E denotes avoided emissions per shared trip, n is the intensity of behavioral nudges, P is the aggregate participation rate, and $\eta > 0$ captures network externalities (Katz & Shapiro, 1985). The term $q(P)$ reflects expected service reliability through the probability of successful matching.

4.3. Aggregate participation, equilibrium and comparative statics

Define the utility differential between multimodal carpooling and private transport:

$$\boldsymbol{\Delta U_i = U_i^C - U_i^T} \quad \textbf{(5)}$$

Let

$$\boldsymbol{\Delta C_i = C_i^C - C_i^T} \quad \textbf{(6)}$$

denote the additional generalized cost of multimodal carpooling relative to individual transport. Substituting (3) and (4), we have :

$$\boldsymbol{\Delta U_i = q(P)(\alpha_i p_c E + \beta_i n + \eta P) - \Delta C_i} \quad \textbf{(7)}$$

An individual adopts multimodal carpooling whenever $\Delta U_i \geq 0$. This condition implies that individuals adopt multimodal carpooling whenever the expected utility gains from incentives, social influences, and network participation exceed the generalized costs associated with multimodal travel and transfer penalties.

[4] Implemented either as a tax (increasing the cost of SOV) or as a reward/subsidy (increasing the benefit of C).

Let P denote the share of individuals choosing carpooling: $P = \Pr(\Delta U_i \geq 0)$. For tractability, assume that:

- $\Delta C_i = \Delta C$ is constant across individuals,
- define $X_i = \beta_i n$

If heterogeneity arises from $\alpha_i \sim F(\alpha)$, the equilibrium participation rate becomes

$$\boldsymbol{P = 1 - F\left(\frac{\Delta C - X - \eta P}{q(P)\, p_c E}\right)} \quad \textbf{(8)}$$

with $q(P)$ defined in (2). Define the mapping

$$\boldsymbol{\Phi(P) = 1 - F\left(\frac{\Delta C - X - \eta P}{q(P)\, p_c E}\right)} \quad \textbf{(9)}$$

An equilibrium participation rate P^*satisfies the fixed-point condition : $P^* = \Phi(P^*)$

Proposition (Existence) : If $F(\cdot)$ is continuous and strictly increasing, then there exists at least one equilibrium $P^* \in [0,1]$. Sketch of proof. The mapping $\Phi(P)$ is continuous and maps the compact convex set $[0,1]$ into itself. Therefore, the existence of at least one fixed point follows from the Brouwer fixed-point theorem (Simon & Blume, 1994).

The equilibrium mapping $\Phi(\mathrm{P})$ is continuous but its monotonicity is not globally guaranteed due to the interaction between network externalities and endogenous matching probabilities. The slope of $\Phi(\mathrm{P})$ is generally ambiguous due to two opposing forces: (i) network externalities, which increase adoption incentives, and (ii) endogenous matching frictions, which reduce the effectiveness of participation incentives. Local monotonicity holds when the marginal gain from network externalities dominates the marginal loss induced by endogenous matching frictions (Mathematical details in Appendix A), i.e. when:

$$\boldsymbol{\frac{\partial}{\partial P}[q(P)\eta P] > -\frac{\partial q(P)}{\partial P}(zpcE + E[\beta]n)} \quad \textbf{(10)}$$

where $z = F^{-1}(1 - P)$ denotes the marginal adopter (i.e., the carbon-incentive sensitivity of the individual who is indifferent between carpooling and private transport), while platform matching efficiency is captured by κ through $q(P) = 1 - e^{-\kappa P}$. And $E[\beta]$ denotes the expectation of β_i under the distribution $F(\beta)$, i.e. the average responsiveness to behavioral nudges in the population. This condition ensures that the equilibrium correspondence is locally increasing in participation, allowing for standard comparative statics around stable equilibria.

Under standard regularity assumptions, $\Phi(P)$ is continuously differentiable and local comparative statics can be derived using the implicit function theorem. Possible equilibrium multiplicity is characterized numerically in Section 6.

4.4. Interpretation: Matching Frictions and Policy Implications

Introducing an endogenous matching probability $q(P)$ transforms multimodal carpooling adoption into a coordination problem. Since the payoff from carpooling is realized only when a match occurs, expected benefits from monetary incentives, behavioral nudges, and social interactions are discounted by the probability of successful matching, which increases with aggregate participation.

With $q(P) = 1 - \exp(-\kappa P)$, matching success is low when participation is limited ($q(P) \approx 0$) and converges to one as the user base expands. The parameter κ captures platform efficiency and determines how quickly reliability improves with participation. A higher value of κ implies that matching efficiency increases more rapidly with P, so that even small increases in participation substantially raise $q(P)$.

In contrast, when κ is low, the matching probability responds only weakly to increases in participation, delaying the point at which the system becomes sufficiently reliable to attract additional users. This mechanism lies at the core of the adoption threshold, understood as the level of participation required for self-sustaining adoption. This generates nonlinear diffusion dynamics: at low participation levels, weak matching prospects reduce adoption incentives and may sustain a low-adoption equilibrium. Conversely, once participation is sufficiently high, improved matching reliability reinforces incentives and network externalities, supporting a high-adoption equilibrium. Hence, equilibrium multiplicity and coordination traps may arise, particularly when κ is low and network effects η are strong. This follows directly from equation (9), where κ affects equilibrium outcomes through its impact on $q(P)$ and thus on the slope of $\Phi(P)$.

From a policy perspective, the model highlights that improving platform efficiency (higher κ) can reduce adoption thresholds and mitigate coordination failures. In this context, the adoption threshold refers to the critical level of aggregate participation P at which carpooling becomes

self-sustaining, i.e., where individual expected utility turns positive for a non-negligible share of the population. It also implies that carbon pricing and behavioral nudges are more effective once a critical mass of participants is reached, suggesting a role for temporary high-intensity interventions during early diffusion stages. This complementarity can be directly seen in equation (7), where both carbon pricing (p_c) and behavioral nudges (n) enter multiplicatively through the same matching probability $q(P)$, implying that their effectiveness is jointly amplified when matching likelihood is high. This coordination mechanism provides the micro-foundation for the tipping dynamics and policy complementarities observed in the equilibrium simulations and calibration results.

5. Empirical Strategy, Calibration, and Identification

5.1. Empirical Roadmap

This section explains how the structural model is disciplined by empirical evidence and subsequently used for counterfactual policy analysis. The empirical strategy proceeds in three steps. First, we calibrate the key structural parameters governing price sensitivity, behavioral responsiveness, network externalities, and platform matching efficiency using a simulation-based method of moments. The calibration targets are chosen to match empirical evidence on: (i) the response of carpooling activity to carbon-related fuel price variation, (ii) the estimated effect of behavioral nudges on adoption probabilities, and (iii) the baseline adoption rate of platform-based carpooling.

Second, we assess the external validity of the calibrated model through an overidentification exercise. Specifically, once the parameter vector $\hat{\theta}$ is obtained, we compute a set of equilibrium model-implied statistics that were not explicitly targeted in the calibration step. These include the equilibrium seat occupancy rate (average number of passengers per matched ride), adoption elasticities with respect to carbon pricing evaluated outside the calibration range, and the incremental adoption response generated by joint policy bundles combining carbon pricing and behavioral nudges. We also compute the implied average CO_2 emissions avoided per trip using emissions factors consistent with French mobility statistics. These simulated outcomes are then compared to independent empirical benchmarks reported in ADEME statistics, the Observatoire du covoiturage, and quasi-experimental evaluations. Model fit is evaluated based on relative prediction errors and whether simulated moments fall within empirically plausible ranges. This validation step provides an external consistency check and ensures that the model does not

merely replicate targeted calibration moments, but also reproduces realistic secondary implications of carpooling adoption and platform performance..

Third, once the parameter vector is calibrated, it is treated as structurally invariant and held fixed. We then perform counterfactual simulations over a broad grid of policy configurations (carbon pricing, nudges, and platform matching efficiency), solving for equilibrium adoption rates as fixed points of the endogenous participation mapping. This allows us to characterize nonlinear adoption dynamics, tipping points, and policy complementarities. Overall, this approach ensures a clear separation between (i) empirical discipline (calibration and validation) and (ii) policy evaluation (counterfactual simulations).

5.2. Data Sources and Empirical Moments

The calibration relies on empirical evidence from French mobility datasets and recent policy evaluations (Olave-Cruz et al. 2025 ; ADEME, 2025 ; Salihou et al. 2023) . We use three main types of empirical moments. First, price-induced variation is documented using quasi-experimental evidence related to carbon taxation and fuel price changes. Existing estimates indicate that fuel price increases associated with carbon pricing lead to an increase in the number of booked seats per route per day. We use this empirical elasticity as a calibration target for the monetary incentive parameter.

Second, behavioral responsiveness is disciplined using experimental evidence on the effect of non-monetary nudges, including informational messages, salience mechanisms, default options, and social norm feedback. Under standard discrete choice models, these effects are typically reported in the form of odds ratios. We exploit these estimates to discipline the behavioral parameter of the model. Third, network effects are disciplined using baseline adoption rates observed in survey data and platform-based measures of carpooling participation in France. While carpooling may occur informally, we focus on platform-mediated adoption, which is the relevant margin for policy design in digital environments such as Mu-CAR.

In addition to these calibration moments, we rely on auxiliary validation moments such as seat occupancy rates and emissions reduction per trip. These additional moments are not targeted in the calibration, but provide external checks on the realism of the calibrated model.

5.3. Structural Parameters and Economic Interpretation

The structural model includes four key parameters:

- α: sensitivity to carbon-related monetary incentives (carbon price or carbon-based reward),
- β: responsiveness to behavioral nudges,
- η: strength of endogenous network externalities (utility gains from aggregate participation),
- κ: matching efficiency of the platform (how quickly matching probabilities increase with participation).

These parameters jointly determine equilibrium adoption through two reinforcing mechanisms. First, pricing incentives and nudges directly shift individual utilities in favor of multimodal carpooling. Second, network externalities and matching frictions generate endogenous adoption dynamics, since participation affects the expected probability of finding a match and therefore the perceived reliability of the service.

5.4. Calibration Method: Simulation-Based Method of Moments

The model does not admit a closed-form expression for equilibrium adoption because individual decisions depend on aggregate participation through matching probabilities and network externalities. We therefore calibrate the parameter vector using a simulation-based method of moments. Let $\theta = (\alpha, \beta, \eta, \kappa)$ denote the vector of structural parameters and let $M(\theta)$ denote the vector of model-implied moments. We choose $\theta$to minimize the weighted distance between simulated and empirical moments:

$$\widehat{\boldsymbol{\theta}} = \mathbf{arg}\ \min_{\boldsymbol{\theta}} \sum_{\boldsymbol{k}} \boldsymbol{w_k} \left(\boldsymbol{M_k^{model}}(\boldsymbol{\theta}) - \boldsymbol{M_k^{data}} \right)^{\mathbf{2}}, \tag{11}$$

where w_k are moment weights. The distribution $F(\theta)$ is assumed to follow a parametric bivariate normal specification and is not estimated non-parametrically. We estimate only the structural parameters $\hat{\theta}$, while the functional form of heterogeneity is imposed. For each candidate parameter vector θ, the model-implied moments $M^{model}(\theta)$ are computed using equilibrium simulations. Specifically, we draw $N = 10{,}000$ heterogeneous agents i with preference parameters $(\alpha_i, \beta_i)$from the assumed distribution $F(\theta)$. Given a policy environment (p_c, n), we compute individual adoption decisions using the structural utility differential $\Delta U_i(P)$, which depends on aggregate participation through network externalities and the

matching probability $q(P) = 1 - \exp(-\kappa P)$. Aggregate participation is then obtained as an equilibrium fixed point $P^*(\theta)$ satisfying $P = \Phi(P)$, where $\Phi(P)$ is the simulated share of adopters. The resulting equilibrium outcomes are used to construct the vector of simulated moments $M^{model}(\theta)$. The SMM objective function is therefore evaluated using equilibrium-consistent predictions rather than partial-equilibrium adoption probabilities.

The calibration is implemented using a machine learning–inspired global search procedure combining grid search and local refinement. Specifically, we first perform a coarse grid search over economically plausible ranges of the parameter vector θ, evaluating the SMM objective function at each grid point using equilibrium simulations. This step ensures global exploration of the parameter space and reduces the risk of convergence to local minima in a highly nonlinear objective function. We then apply a local refinement step around the best-performing candidate using a derivative-free optimization algorithm (Nelder–Mead simplex search), which iteratively improves the fit by exploring nearby parameter configurations without requiring gradient information. This two-step procedure is well-suited to structural models with equilibrium constraints, as the objective function is non-smooth and evaluated through computational fixed-point solutions.

5.5. Empirical anchoring

Parameters are externally calibrated using empirical benchmarks drawn from multiple sources. This approach does not constitute a unified structural estimation based on a single micro-dataset, but it ensures that the simulated economy reproduces realistic orders of magnitude for adoption rates, elasticities, and matching outcomes. Each parameter is disciplined by a distinct empirical margin, limiting confounding.

Price sensitivity (α). α is calibrated to match quasi-experimental evidence on the response of carpooling activity to fuel price changes induced by carbon taxation (Olave-Cruz et al., 2025).

Behavioral responsiveness (β). β is anchored using experimental evidence on nudges (Salihou et al., 2023). In a random utility logit framework, experimental effects are typically reported as odds ratios. Since logit choice probabilities imply that utility differences map into log-odds, we recover the structural utility coefficient as β = ln(OR), ensuring consistency between experimental estimates and the underlying discrete choice model.

Network externalities (η). η is calibrated to reproduce the baseline platform-based adoption rate reported in French mobility statistics (ADEME, 2025)

Matching efficiency (κ). κ is calibrated using external evidence on matching success and seat occupancy from French carpooling statistics (ADEME, 2025). Mu-CAR will provide direct estimates of κ from realized match probabilities conditional on participation once the platform is deployed.

5.6. Calibration Results and Model Fit

Table 1 summarizes calibration targets, validation moments, and auxiliary assumptions. Panel A reports the targeted moments used in calibration. Panel B reports additional validation moments used to assess external consistency. Panel C reports auxiliary parameters and modeling assumptions. The calibrated model reproduces the main targeted moments: the empirical response of booked seats to carbon pricing, the odds ratio associated with behavioral nudges, and the baseline platform-based adoption rate. Importantly, the model also reproduces several untargeted validation moments through the overidentification exercise described in Section 5.1. In particular, equilibrium simulations based on the calibrated parameter vector generate predictions for average seat occupancy and CO_2 emissions reductions per trip, which are not used in the calibration step. These simulated outcomes are then compared ex post to independent empirical benchmarks from ADEME and the Observatoire du covoiturage. The close correspondence in orders of magnitude supports the external validity and empirical plausibility of the structural framework.

5.7. Local sensitivity and moment informativeness

A common concern in simulation-based calibration is weak identification when the number of moments is limited relative to the number of parameters. We address this concern in three ways. First, calibration exploits orthogonal empirical sources: carbon price variation informs α, experimental odds ratios inform β, baseline adoption rates inform η, and matching performance informs κ. These moments are based on distinct empirical sources and exploit variation originating from different economic mechanisms, thereby limiting redundancy in the identifying information across parameters. Second, the mapping between moments and parameters is structurally transparent. In particular, the logit mapping from odds ratios to β is

direct, leaving little ambiguity. Third, we verify numerically that the Jacobian matrix of the moment mapping is locally full rank around the calibrated parameter vector: $J(\theta) = \frac{\partial M(\theta)}{\partial \theta'}$.

This suggests that the targeted moments are locally informative about parameters in the neighborhood of the calibrated vector (Hansen, 1982; Newey and McFadden, 1994; Aguirregabiria and Mira, 2010). Additional robustness checks conduct a local sensitivity analysis around the calibrated parameter vector $\hat{\theta}$. Specifically, we perturb the calibration moments within empirically plausible ranges (reflecting reported standard errors or confidence intervals) and recompute the implied equilibrium outcomes. This exercise does not involve re-estimating the model on alternative datasets, but rather evaluates the stability of the calibrated solution with respect to measurement uncertainty in the target moments. The results indicate that moderate perturbations do not materially affect the model's main qualitative predictions, particularly regarding tipping dynamics and policy complementarities.

Table 1 . Model Calibration, Validation, and Overidentification

			Panel A. Calibration Targets		
Moment / Prediction	**Data**	**Model**	**Error**	**Targeted**	**Sou**
Carbon pricing range (P_c)	7–100 €/tCO₂	—	—	✓	Olave-Cruz
Change in booked seats (α_i)	1.2–1.5	1.30	+0.10	✓	Olave-Cruz
Odds ratio (nudges) (β_i)	1.94	1.94	0.00	✓	Salihou et
Baseline adoption rate (η)	18%	17.8%	-0.2 pp	✓	ADEMI
			Panel B. Validation and Overidentification		
Seat occupancy rate (r)	2.17	2.05	-0.12	✗	Observatoire du ADEMI
Elasticity outside tax range	-0.35	-0.32	+0.03	✗	Liter
Odds ratio (combined policies)	2–3	2.4	0 (within range)	✗	Salihou et
Emissions reduction per trip (E)	37.2 kg	36.5 kg	-0.7	✗	ADEMI
			Panel C. Model Assumptions and Auxiliary Parameters		
Parameter	**Value**	**Range**	**Source / Justification**		**C**
Incentive sharing parameter (λ)	0.70	[0.5 – 0.8]	Platform economics / shared mobility		Determines s
Matching efficiency (κ)	Calibrated	—	ADEME (2025); Observatoire du covoiturage (French carpooling statistics)		Externally calibrated to match observ future Mu-CAR data will allow dir

Notes : Seat occupancy is an endogenous aggregate moment implied by the equilibrium matching process rather than a primitiv modeled at the individual decision level but is derived from equilibrium outcomes of the matching process, computed ex post in transported to the number of successfully matched vehicles.

6. Structural Simulation Framework

6.1.. Objective and Key Principle

The goal of this section is to quantify how equilibrium carpooling adoption responds to policy instruments in the presence of endogenous network effects and matching frictions. A key principle is that all counterfactual analysis is performed under a fixed calibrated structural environment. Once the parameter vector $\hat{\theta} = (\hat{\alpha}, \hat{\beta}, \hat{\eta}, \hat{\kappa})$ is obtained in Section 5, it is held constant throughout all simulations. Policy scenarios differ only through policy instruments (carbon pricing, behavioral nudges, and platform efficiency), not through behavioral parameters.

We simulate a population of $N = 10{,}000$ heterogeneous individuals indexed by i. Each agent is characterized by preference parameters (α_i, β_i), drawn from the calibrated distribution $F(\theta)$.

$\alpha_i \sim \mathcal{N}(\mu_\alpha, \sigma_\alpha^2), \beta_i \sim \mathcal{N}(\mu_\beta, \sigma_\beta^2),$

and we assume independence between $\alpha_i$and β_i. The joint distribution $F(\theta)$ is therefore the implied bivariate normal distribution. Agents differ in their sensitivity to monetary incentives and behavioral interventions. For each policy configuration, individuals choose between private transport and multimodal carpooling by comparing utilities derived from the structural model.

The same simulation framework with $N = 10{,}000$ agents is used in both stages of the analysis. In the first step, it is embedded within the SMM calibration to compute equilibrium moments and estimate $\hat{\theta}$. In the second step, the calibrated parameter vector is held fixed and the framework is used for counterfactual policy experiments. The only difference between the two stages is whether parameters are estimated or kept fixed for policy evaluation.

6.2. Endogenous Equilibrium Adoption as a Fixed Point

Because individual adoption depends on P through both network effects (ηP) and matching probabilities $q(P)$, aggregate participation must satisfy a fixed-point condition. For any candidate participation rate P, the model implies an adoption share:

$$\boldsymbol{\Phi(P) = \frac{1}{N}\sum_{i=1}^{N} \mathbf{1}\,[\Delta U_i(P) \geq 0]}. \qquad \textbf{(12)}$$

An equilibrium adoption rate $P^*$is defined as: $P^* = \Phi(P^*)$. This equilibrium may be unique or multiple depending on parameter values. In particular, strong network effects and weak matching efficiency may generate coordination failures and tipping points, where adoption remains trapped in a low-participation regime unless policy interventions are sufficiently strong.

6.3. Fixed-Point Algorithm and Equilibrium Selection

For each policy configuration, we compute the equilibrium adoption rate P^* by solving the fixed-point condition $P = \Phi(P)$. Starting from an initial guess $P^{(0)}$, we iterate:

$$\boldsymbol{P^{(t+1)} = \Phi\left(P^{(t)}\right)} \quad \textbf{(13)}$$

We declare convergence when the distance between two successive iterates satisfies $| P^{(t+1)} - P^{(t)} | < 10^{-3}$. This tolerance level is standard in numerical fixed-point algorithms and implies that the equilibrium participation rate is computed with an accuracy of 0.1 percentage point, while keeping computation time manageable, or until reaching a maximum number of iterations $T_{\max} = 10{,}000$. Note that t denotes the iteration index of the fixed-point algorithm, while $N = 10{,}000$ refers to the number of simulated individuals used to approximate the adoption mapping $\Phi(P)$.

Because adoption depends endogenously on aggregate participation through both network externalities and matching success, equilibrium carpooling adoption is characterized as a fixed point $P = \Phi(P)$. The nonlinearity induced by the matching technology $q(P) = 1 - e^{-\kappa P}$ implies that $\Phi(P)$ may intersect the 45-degree line multiple times, generating a low-adoption equilibrium, a high-adoption equilibrium, and an intermediate unstable tipping threshold. To clarify equilibrium selection, we interpret the computation as an adaptive participation dynamic $P^{(t+1)} = \Phi(P^{(t)})$, consistent with gradual learning about platform reliability. A fixed point $P^*$is locally stable if $| \Phi'(P^*) | < 1$, while unstable equilibria cannot persist under small perturbations. This condition follows from the standard local stability criterion of the iterative mapping: linearizing around P^*implies $P^{(t+1)} - P^* \approx \Phi'(P^*)(P^{(t)} - P^*)$, so convergence requires $| \Phi'(P^*) | < 1$.

When multiplicity arises, the selected equilibrium depends on initial conditions, implying basin-of-attraction effects and hysteresis: policies must push participation beyond the unstable

threshold to trigger convergence toward the high-adoption regime. In simulations, equilibrium adoption is obtained by iterating $P^{(t+1)} = \Phi(P^{(t)})$ until convergence, initializing at the calibrated baseline participation rate. Robustness checks using alternative initializations $P^{(0)} \in [0,1]$, including both interior and boundary starting values confirm tipping dynamics and quantify path dependence.

The converged value is taken as the stable equilibrium adoption rate P^*. When multiple equilibria exist, the algorithm converges to the locally stable equilibrium associated with the chosen initial condition. Unless otherwise stated, we initialize the algorithm at the baseline adoption level implied by the calibrated model.

6.4. Policy Grid and Simulated Dataset

We generate a balanced simulated dataset covering a broad policy space. The grid is defined by:

- carbon price: $p_c \in [0,95]$with step size 5,
- behavioral nudges: $n \in [0,1.8]$with step size 0.2,
- matching efficiency: $\kappa \in [0.5,5]$ with unit increments.

This design produces 2,000 policy configurations. For each configuration, we compute the equilibrium adoption rate P^*. This yields a dataset suitable for analyzing nonlinear responses, policy complementarities, and threshold effects. Table 2 reports summary statistics. Equilibrium adoption ranges from 2.2% to 98%, indicating strong nonlinear adoption dynamics across the policy space. $P^*$is the equilibrium share of individuals using multimodal carpooling under a given policy scenario.

Table 2. Summary Statistics of the Simulated Equilibrium Dataset

Variable	Obs	Mean	Std. Dev.	Min	Max
Equilibrium adoption rate P^*	2000	0.2538	0.3809	0.0223	0.98
Carbon price (p_c)	2000	47.5	28.83	0	95
Behavioral nudge	2000	0.9	0.574	0	1.8
Matching efficiency (κ)	2000	2.75	1.43	0,5	5

7. Simulation Results

7.1. Baseline Reduced-Form Approximation of the Equilibrium Mapping

To provide a compact summary of the simulated equilibrium outcomes, we estimate simple reduced-form approximations of the equilibrium adoption mapping $P^*(p_c, n, \kappa)$. Specifically, we regress the simulated equilibrium adoption rate on the policy instruments using the following linear projection:

$$\boldsymbol{P^* = a + b_1 p_c + b_2 n + b_3 \kappa + \varepsilon,} \quad \textbf{(14)}$$

and we extend this specification with interaction terms and quadratic terms in order to capture complementarities and curvature in the equilibrium response surface. It is important to emphasize that these regressions are not econometric estimates based on observational data. Instead, they should be interpreted as numerical approximations of the equilibrium mapping generated by the structural model. The estimated coefficients therefore summarize the average direction and magnitude of policy effects over the simulated policy grid, but they do not constitute structural parameters and should not be interpreted as causal estimates in the usual statistical sense.

Appendix[5] B reports the resulting projections. Standard errors are reported as measures of goodness-of-fit of the polynomial approximation and should not be interpreted as sampling uncertainty. The reduced-form projections confirm that all three policy levers—carbon pricing, behavioral nudges, and matching efficiency—are positively associated with equilibrium adoption. In specification (1), the coefficients on p_c, n, and κ are all positive, indicating that increasing any of these instruments shifts the equilibrium toward higher participation.

Specification (2) introduces interaction terms and reveals strong complementarity effects. In particular, the positive coefficients on $p_c \times n$ and $p_c \times \kappa$ suggest that the marginal impact of carbon pricing is amplified when nudges are stronger and when the platform achieves higher matching efficiency. Likewise, the positive coefficient on $n \times \kappa$ indicates that behavioral interventions become substantially more effective when matching reliability improves. These

[5] The results are obtained from simulations of a calibrated structural model rather than econometric estimation on observed data. In this setting, p-values and statistical significance are not applicable, as outcomes are deterministic conditional on the calibrated parameters. The reported results reflect model-implied mechanisms rather than statistical inference.

interaction patterns are consistent with the core mechanism of the model: pricing and nudges increase participation, which improves matching success and reinforces network effects, generating nonlinear amplification. Specification (3) further supports the presence of nonlinearities through positive curvature terms. This suggests that adoption responses may be convex over parts of the policy space, which is consistent with tipping dynamics: once participation approaches a critical mass, marginal policy changes can generate disproportionately large equilibrium shifts.

Overall, Table 3 provides a useful descriptive summary of the simulated equilibrium dataset. However, these linear and polynomial projections necessarily abstract from the full nonlinear fixed-point structure of the model. The next section therefore turns to the full equilibrium analysis, focusing explicitly on threshold effects, coordination traps, and the emergence of multiple steady states driven by network externalities and endogenous matching.

7.2. Equilibrium results

Figure 1 illustrates a highly nonlinear relationship between carbon pricing and the equilibrium adoption rate of multimodal carpooling. At low carbon price levels (0–30 €/tCO_2), equilibrium adoption remains close to zero in both scenarios (i.e. with or without nudge), suggesting that weak monetary incentives are insufficient to overcome generalized costs, behavioral inertia, and coordination frictions in the matching process. However, beyond a critical threshold, adoption rises abruptly, revealing a clear tipping-point mechanism driven by network externalities and endogenous matching. Without behavioral intervention, the tipping point occurs around 50–55 €/tCO_2, where adoption jumps sharply from near zero to above 50%, and then continues to increase gradually as carbon prices rise further.

By contrast, introducing a behavioral nudge significantly shifts the tipping point to the left. Adoption increases dramatically already around 35 €/tCO_2, reaching roughly 60% immediately after the threshold and exceeding 80% by 50 €/tCO_2. This indicates that nudges facilitate early coordination and reduce the level of carbon pricing required to trigger the transition toward a high-adoption equilibrium. At higher carbon prices (above 70–80 €/tCO_2), adoption in both scenarios converges toward saturation, although the nudge scenario remains systematically higher. This suggests that behavioral interventions are most effective in the intermediate price range, where low participation limits matching success, creating a self-reinforcing barrier to adoption.

Overall, the figure provides strong evidence of complementarity between carbon pricing and behavioral nudges: while carbon pricing alone can eventually induce large-scale adoption, combining monetary incentives with behavioral tools accelerates diffusion dynamics and substantially lowers the carbon price needed to achieve mass participation.

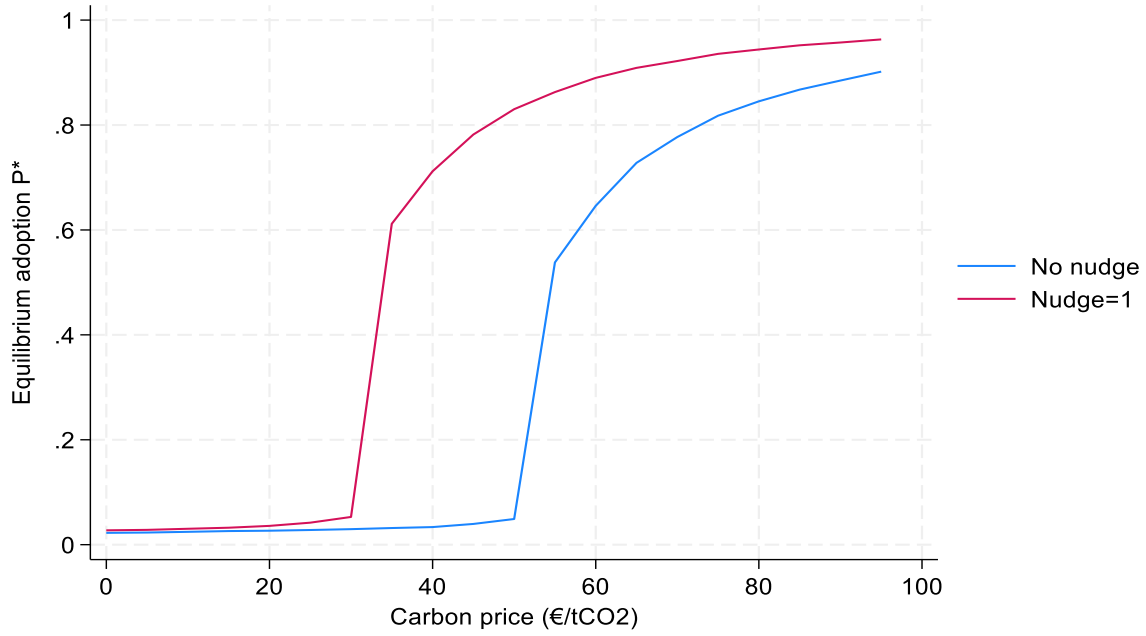

Figure 1. Carbon Pricing, Behavioral Nudges, and Tipping Dynamics in Equilibrium Carpooling Adoption

Figure 2 and Appendix C provide a comprehensive visualization of the equilibrium adoption surface P^*as a joint function of carbon pricing and behavioral nudges. Both figures reveal a sharply nonlinear transition between two distinct regimes: a low-adoption equilibrium (blue area) where multimodal carpooling remains marginal, and a high-adoption equilibrium (red area) where adoption becomes quasi-universal. The boundary separating these regimes is steep and clearly downward sloping, indicating that behavioral nudges substantially reduce the carbon price required to trigger large-scale adoption. In particular, when nudges are weak, only high carbon prices are able to overcome generalized costs and matching uncertainty, whereas stronger nudges shift the system toward mass participation even under moderate pricing.

This pattern provides direct evidence of strong policy complementarity: nudges act as a coordination device that accelerates the accumulation of users, improves matching probabilities, and amplifies network externalities. Importantly, the presence of large low-adoption zones also highlights the existence of coordination failures: when both policy instruments remain below critical thresholds, the system becomes trapped in a stable

equilibrium with persistently low participation. Overall, these figures confirm that incremental or isolated interventions are unlikely to deliver substantial adoption gains, while coordinated pricing–behavioral packages can unlock tipping dynamics and rapidly move the system toward a high-adoption equilibrium.

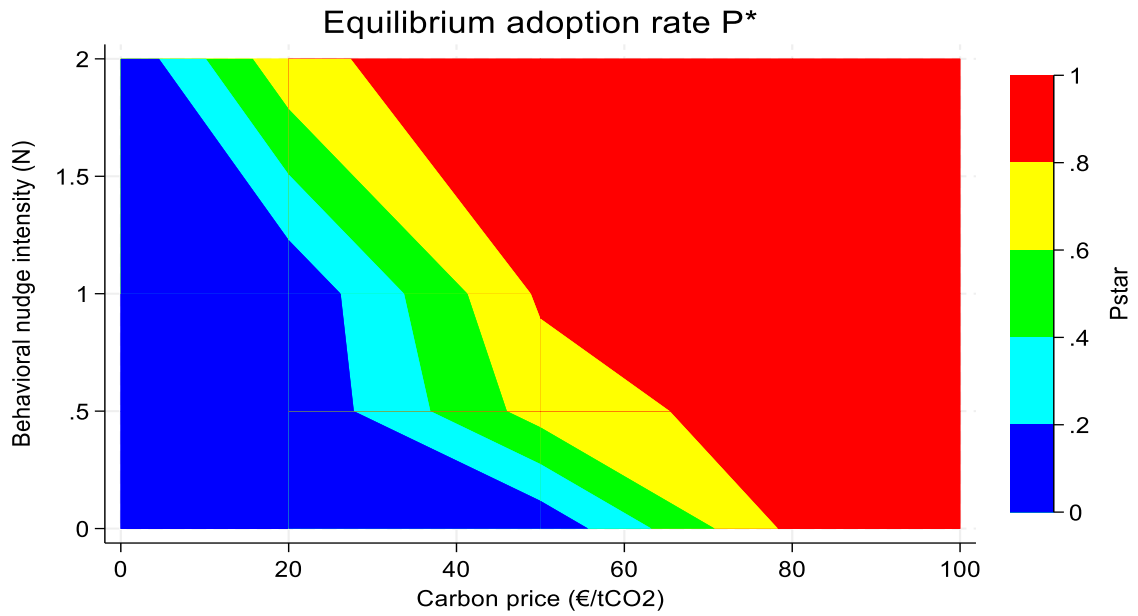

Figure 2. Carbon Pricing–Nudge Complementarity and Threshold Effects in Equilibrium Adoption

7.3. Behavioral Nudges as Implicit Carbon Pricing: A Structural Policy Mapping

Figures 3–4 translate behavioral nudges into an implicit carbon price equivalent, defined as:

$$\Delta p_c = p_c(n = 0) - p_c(n = 1), \quad \textbf{(15)}$$

i.e., the reduction in carbon pricing required to reach the same equilibrium adoption target P^* when a full-strength nudge is implemented. The implicit carbon price should be interpreted as a policy-equivalence metric within the model, rather than a welfare-based valuation. The heatmap indicates that the implicit carbon value of nudges lies mostly between 20 and 30 €/tCO_2, implying that behavioral interventions can substitute for a substantial share of monetary incentives. This equivalence is intrinsically shaped by the model's endogenous diffusion mechanism.

Since adoption benefits are weighted by the matching probability $q(P) = 1 - \exp(-\kappa P)$, nudges are more effective when matching efficiency κ is high. The slight increase in Δp_c with κ therefore reveals strong complementarity between behavioral interventions and platform performance: better matching raises the extent to which nudges translate into realized participation. More fundamentally, the nonlinear structure of Δp_c reflects multiple equilibria and tipping dynamics. Because both network effects (ηP) and matching success $q(P)$ increase with aggregate participation, the system may remain trapped in a low-adoption equilibrium unless incentives are strong enough to cross a critical mass threshold.

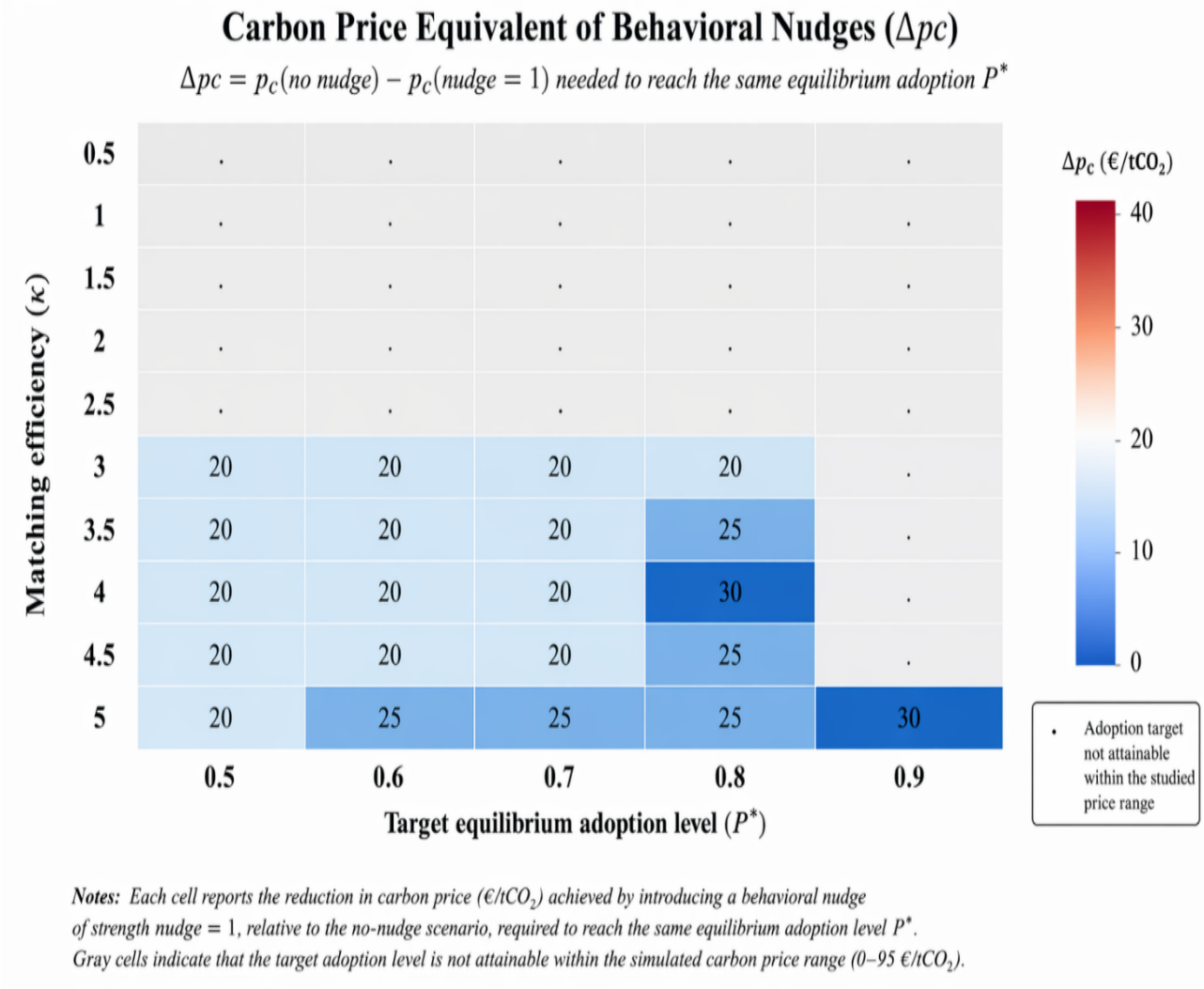

Figure 3. Heatmap of the Implicit Carbon Price of Behavioral Nudges *(Δp_c)*

Nudges operate precisely by shifting this threshold, lowering the carbon price required to trigger an adoption cascade toward the high-participation equilibrium. The infeasible regions further highlight that, under severe matching frictions, neither pricing nor nudges can achieve ambitious adoption targets without improvements in platform efficiency. This implicit carbon

price should be interpreted as a model-consistent shadow value conditional on the calibrated structural environment, rather than as a universal monetary valuation.

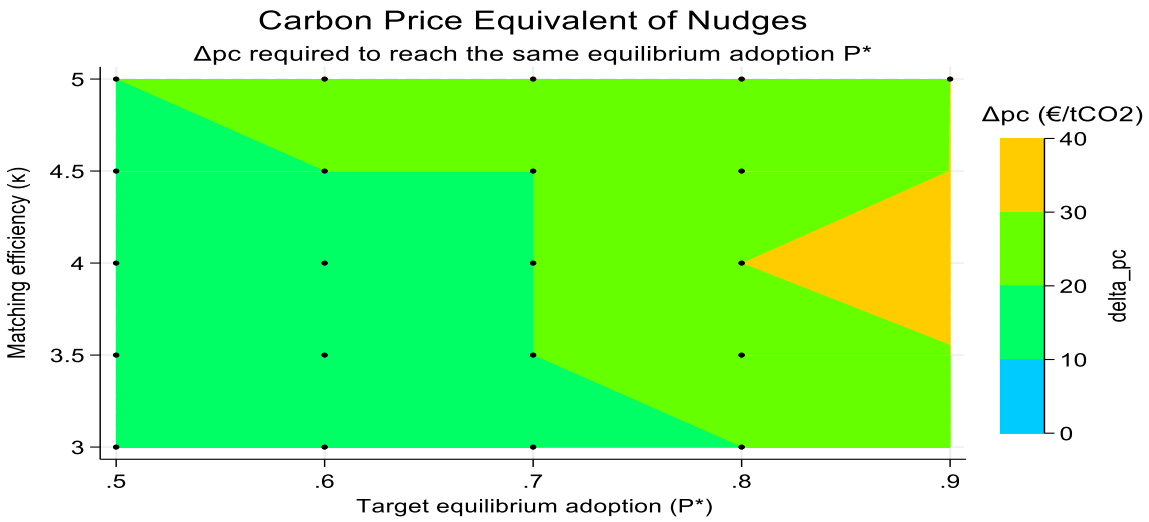

Figure 4. Structural Policy Surface: Implicit Carbon Price of Nudges Across Adoption Targets and Matching Efficiency

8. Robustness Checks & Sensitivity Analysis

Result 1 (tipping): Nudges significantly shift the critical carbon price required to trigger a high-adoption equilibrium.

The figure 5 highlights the presence of tipping dynamics and a well-defined critical carbon price p_c^{crit} required to reach a high-adoption equilibrium ($P^* \geq 0.8$). In the absence of nudges, the threshold remains high—around 75–85 €/tCO₂—indicating that the system can be trapped in a low-adoption equilibrium due to coordination failures. Introducing a behavioral nudge ($n = 1$) substantially shifts this threshold downward, reducing p_c^{crit} to approximately 50–65 €/tCO₂, depending on matching efficiency. The figure 5 also confirms that higher platform efficiency (κ) systematically lowers the threshold, consistent with the endogenous matching channel $q(P) = 1 - \exp(-\kappa P)$. Overall, the results provide clear evidence that nudges act as a coordination device, significantly reducing the carbon price required to trigger a transition toward the high-adoption equilibrium, especially when matching efficiency is sufficiently strong.

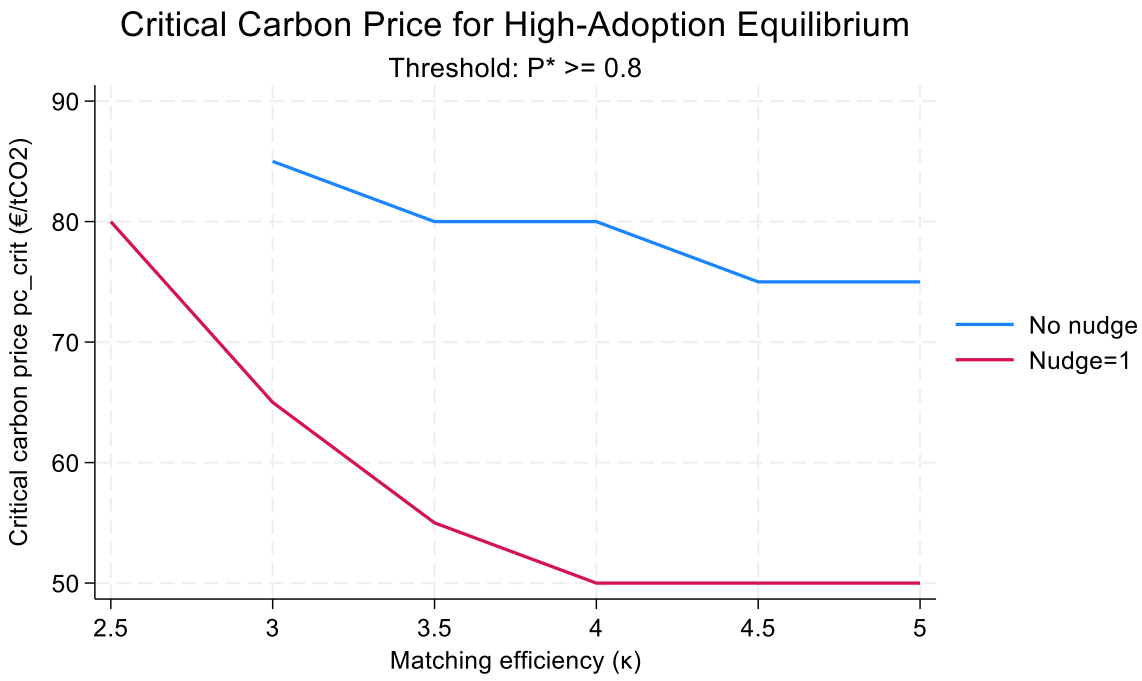

Figure 5. Critical Carbon Price for Reaching the High-Adoption Equilibrium ($P \geq 0.8$)*

Result 2 (local effects): Policy impacts are highly nonlinear and concentrated around tipping regions

Figure 6 complements Figure 1 by reporting the *local policy responsiveness* of equilibrium adoption to carbon pricing, measured by the derivative $\frac{dP^*}{dp_c}$ under high matching efficiency ($\kappa = 5$). While Figure 1 documents the existence of adoption thresholds, Figure 6 shows that the effectiveness of carbon pricing is highly concentrated within a narrow region around the tipping point. Marginal effects are close to zero at low carbon prices, then rise sharply and peak near the unstable equilibrium, before collapsing again once the high-adoption regime is reached. This pattern implies that carbon pricing operates mainly as a trigger mechanism rather than a smooth incentive: below the threshold, price changes have little impact, whereas near the tipping region small increases generate large adoption responses. Nudges shift this high-sensitivity region leftward, confirming that behavioral interventions primarily reduce the critical coordination threshold rather than increasing adoption uniformly across the policy space.

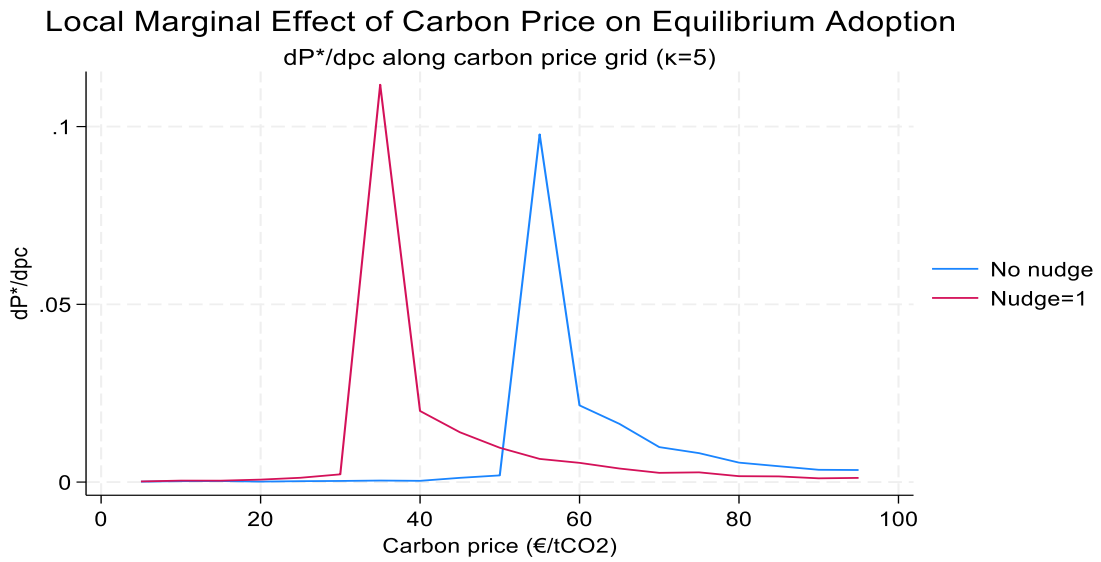

Figure 6. Nonlinear Marginal Effects of Carbon Pricing Around the Tipping Region (κ = 5)

Result 3 (robustness): The tipping dynamics and equivalence measures remain robust across alternative thresholds.

Figure 7 reports how behavioral nudge intensity affects the critical carbon price required to reach adoption tipping points. Each panel corresponds to a specific combination of the adoption threshold $P^*$and the matching efficiency parameter κ. The parameter κgoverns the matching technology $q(P) = 1 - e^{-\kappa P}$, where higher values correspond to more efficient conversion of behavioral nudges into adoption.

To read the figure, each panel should be interpreted as holding (P^*, κ) fixed, while tracing how nudges shift the critical carbon price. The numbers displayed in each panel indicate the parameter configuration of that subplot. The figure should therefore be interpreted as a comparative statics exercise over behavioral and technological parameters. Across all configurations, higher nudge intensity reduces the required carbon price, while higher matching efficiency shifts the entire schedule downward. These patterns are robust across adoption thresholds, confirming that the tipping dynamics are structural features of the model

.

.

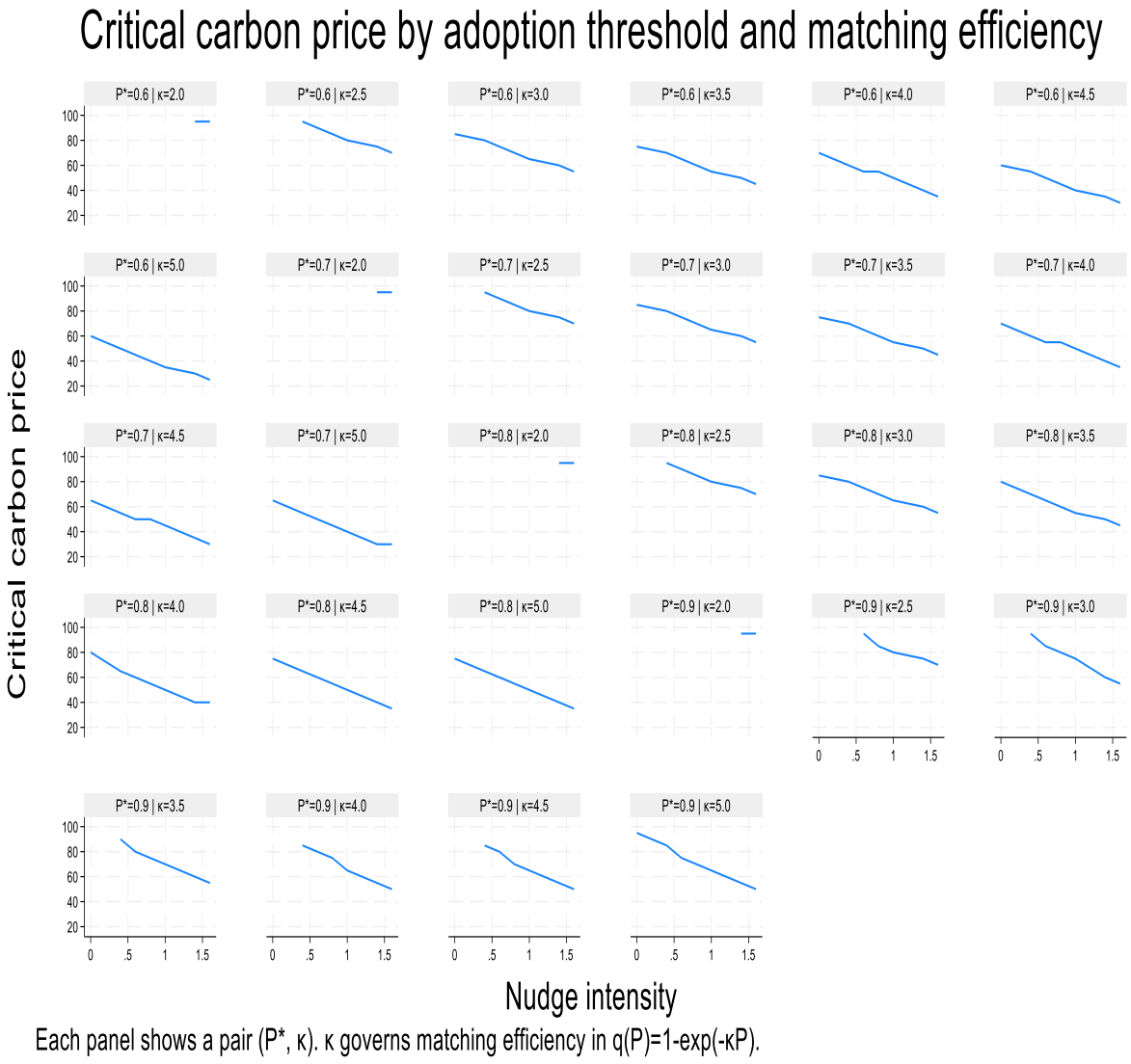

Figure 7. Critical carbon prices under behavioral nudges: reading thresholds and matching efficiency

Results 4 — Policy frontier: min pc for each nudge (given target P)*

Figure 8 depicts a conditional policy trade-off frontier linking behavioral nudges and carbon pricing, defined as the minimum carbon price required to reach a target equilibrium adoption level $P^* = 0.8$, given high matching efficiency ($\kappa = 5$). The frontier is strictly downward sloping, indicating that stronger nudges reduce the carbon price required to achieve a fixed adoption objective. Quantitatively, in the absence of nudges, reaching $P^* = 0.8$ requires a carbon price close to 75 €/tCO₂, whereas increasing nudge intensity lowers this requirement to roughly 30 €/tCO₂ at high nudge levels.

Importantly, this trade-off is conditional on the adoption target and platform efficiency and does not contradict the complementarity effects documented in Figure 1. In particular, carbon pricing and nudges remain complementary in the sense that, for a given carbon price, increasing nudge intensity raises equilibrium adoption and can shift the system across the tipping region. Overall, the figure provides a policy-relevant mapping of instrument combinations that jointly deliver a high-adoption equilibrium, offering a practical tool for designing cost-effective policy packages that balance monetary and behavioral interventions.

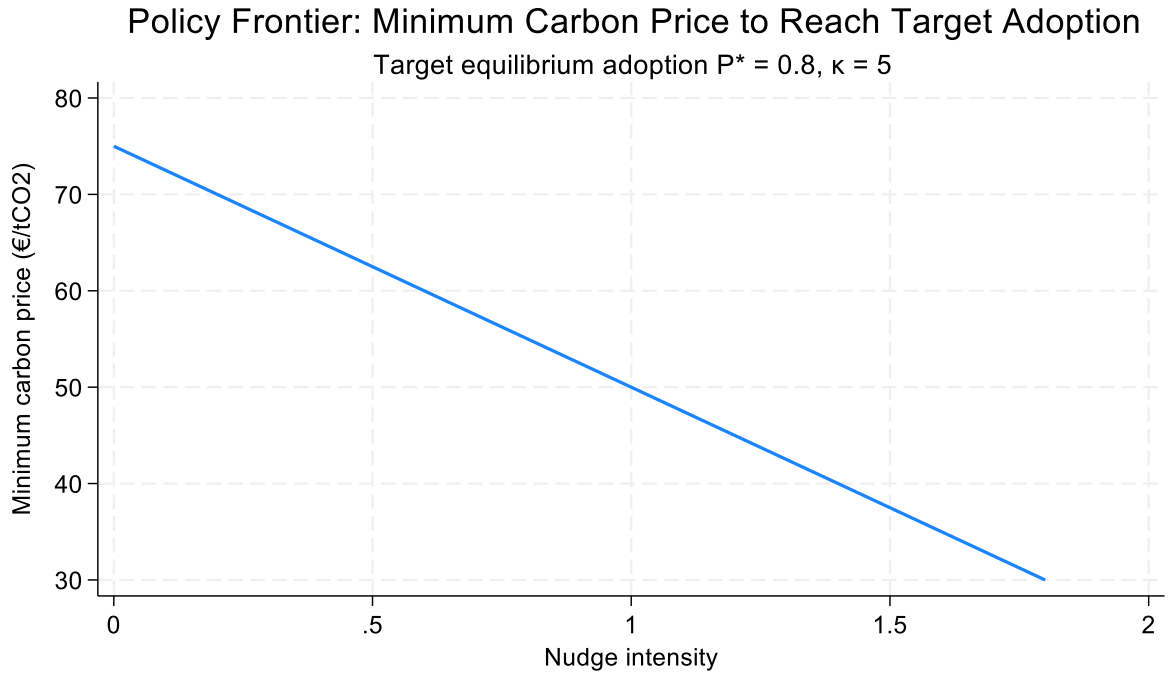

Figure 8. Carbon Price–Nudge Trade-Off Frontier for Achieving High Adoption (P = 0.8)*

9. Conclusion

This paper develops a unified structural framework to study multimodal carpooling adoption in France under three central policy and market mechanisms: carbon pricing**,** behavioral nudges**,** and endogenous network effects driven by platform matching efficiency. The model formalizes carpooling adoption as a coordination problem in which individual willingness to participate depends not only on private costs and incentives, but also on the expected probability of successfully finding a match. This participation-dependent matching channel generates nonlinear diffusion dynamics, including threshold effects**,** multiple equilibria, and the possibility of persistent low-adoption traps.

The simulation results highlight several key policy implications. First, carbon pricing increases adoption, but its effectiveness is strongly limited by coordination failures when participation remains low. In such contexts, moderate carbon prices may have almost no impact because individuals anticipate low matching success, keeping the system stuck in a stable low-adoption equilibrium. Second, behavioral nudges significantly reduce the critical threshold required to trigger mass adoption. By shifting perceived utility and encouraging early participation, nudges operate as a coordination mechanism that accelerates entry into the high-adoption regime. This generates strong complementarity: nudges amplify the impact of carbon pricing precisely where network effects are strongest—near tipping points. Third, the analysis shows that platform design and matching efficiency are decisive structural parameters**.** Improvements in matching performance (higher κ) reduce uncertainty, strengthen network feedback loops, and determine whether adoption converges toward widespread diffusion or remains trapped in low participation.

A central contribution of the paper is the introduction of an implicit carbon price equivalence of behavioral nudges. The results suggest that nudges can substitute for a substantial portion of monetary incentives, with an estimated equivalent value typically between 20 and 30 €/tCO_2, though this value depends critically on matching efficiency and equilibrium regime. At the same time, nudges also act as complements to carbon pricing: by shifting participation incentives and lowering coordination thresholds, they amplify the marginal effectiveness of carbon pricing near tipping points and help the system converge toward higher-adoption equilibria.

This provides policymakers with a practical metric for comparing behavioral interventions to conventional pricing instruments within a consistent structural environment. Overall, the findings emphasize that scaling multimodal carpooling requires more than isolated marginal interventions. Effective decarbonization policy must be designed as a coordinated package, combining pricing instruments, behavioral strategies, and platform improvements. In particular, policy success depends on the ability to push adoption beyond critical mass thresholds, where network effects and improved matching generate self-reinforcing diffusion dynamics.

Finally, the Mu-CAR project will provide a unique empirical opportunity to validate and structurally estimate the model using real-world experimental variation. By linking theoretical equilibrium dynamics with platform-based mobility data, the framework offers a scalable tool for designing evidence-based transport policies capable of triggering durable transitions toward low-carbon shared mobility.

Acknowledgements

This work was supported by the Mu-CAR project, funded by the Bourgogne–Franche-Comté Region in France.

Appendix A. Derivation of equilibrium properties and condition (10)

A.1 Equilibrium mapping

From individual utility maximization, the participation condition is:

$$\Delta U_i = q(P)(\alpha_i p_c E + \beta_i n + \eta P) - \Delta C$$

Let:

$$z_i = \alpha_i$$

Then individuals adopt if:

$$z_i \geq \frac{\Delta C - X - \eta P}{q(P)\, p_c E}$$

Hence:

$$P = 1 - F\left(\frac{\Delta C - X - \eta P}{q(P)\, p_c E}\right)$$

Define:

$$Z(P) = \frac{\Delta C - X - \eta P}{q(P)\, p_c E}$$

So:

$$\Phi(P) = 1 - F(Z(P))$$

A.2 Derivative of the equilibrium mapping

Differentiate:

$$\frac{d\Phi(P)}{dP} = -f(Z(P)) \cdot Z'(P)$$

Compute $Z'(P)$:

$$Z'(P) = \frac{-\eta q(P) - (\Delta C - X - \eta P) q'(P)}{(q(P))^2 p_c E}$$

Thus:

$$\frac{d\Phi(P)}{dP} = \frac{f(Z(P))}{(q(P))^2 p_c E}\left[\eta q(P) + (\Delta C - X - \eta P)\, q'(P)\right]$$

A.3 Local monotonicity condition

Since $f(\cdot) > 0$, the sign of $\frac{d\Phi}{dP}$is determined by:

$$\eta q(P) + (\Delta C - X - \eta P)\, q'(P)$$

Define marginal adopter threshold:

$$z = F^{-1}(1 - P)$$

Using:

$$\Delta C - X - \eta P = z\, q(P)\, p_c E$$

Substituting yields:

$$\eta q(P) + q'(P)\, z\, q(P)\, p_c E > 0$$

Rearranging gives condition (10):

$$\frac{\partial}{\partial P}[q(P)\eta P] > -q'(P)\,(z p_c E + E[\beta] n)$$

A.4 Role of matching technology

With:

$$q(P) = 1 - e^{-\kappa P}, q'(P) = \kappa e^{-\kappa P}$$

we obtain:

- diminishing marginal matching returns
- nonlinear amplification of network effects
- possible non-monotonic Φ(P)

A.5 Regularity and fixed points

Under standard assumptions:

- F(·) continuous and strictly increasing
- q(P) continuously differentiable

- bounded support of heterogeneity

Φ(P) is continuous on [0,1], ensuring existence of at least one fixed point (Brouwer). Local uniqueness depends on condition (10).

Appendix B. Polynomial Projections of the Simulated Equilibrium Adoption Surface

Variables	(1)Baseline Linear Projection	(2) Interaction Projection	(3) Quadratic Projection
Carbon price (p_c)	0.0068	—	—
	(0.0001)		
Behavioral nudge (nudge)	0.125	—	—
	(0.0821)		
Matching efficiency (κ)	0.139	—	—
Constant	-0.130	—	—
	(0.110)		
p_c × κ	—	0.0024	—
		(0.0000)	
p_c × nudge	—	0.0005	—
		(0.0001)	
nudge × κ	—	0.0348	—
		(0.0023)	
Constant	—	-0.1804	—
		(0.0076)	
p_c^2	—	—	0.00007
			(1.94)
$nudge^2$	—	—	0.0656
			(0.0051)
κ^2	—	—	0.0245
			(0.0006)
Constant	—	—	-0.274
	Model fit statistics		
	(1) Baseline OLS	**(2) Interaction OLS**	**(3) squared variable OLS**

Observations	2000	2000	2000
R^2	0.5835	0.736	0.5825
Adjusted R^2	0.5829	0.735	0.5818
Root MSE	0.24602	0.19579	0.24632

Appendix C . Iso-Adoption Contours: Trade-Offs between Carbon Pricing and Behavioral Nudges

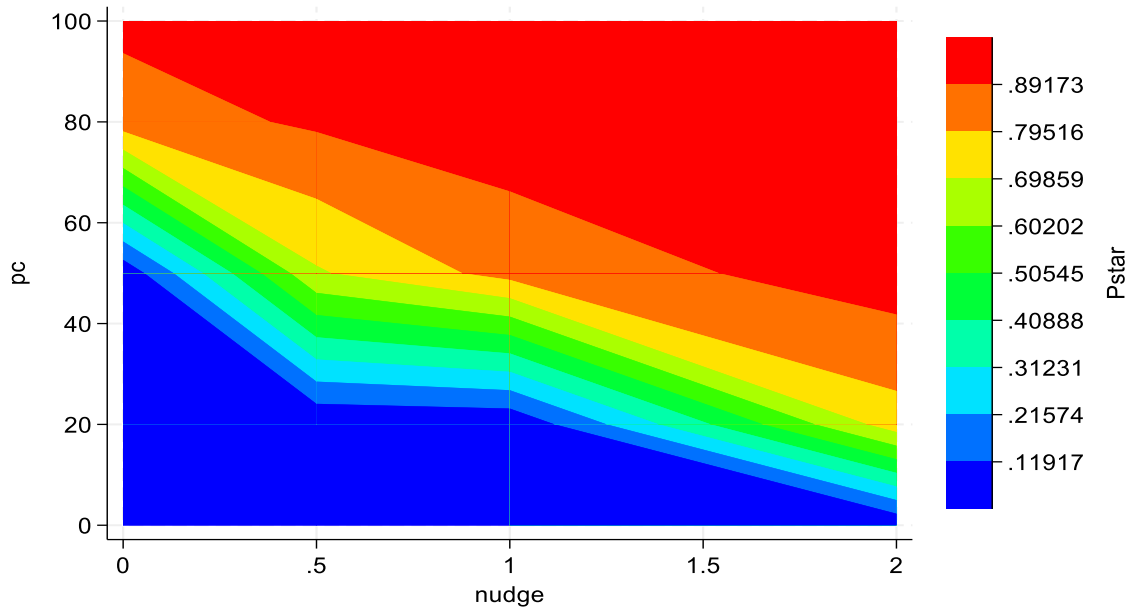

References

ADEME., 2025.Qualifier et quantifier l'offre et la demande de covoiturage en France. Rapport final

Aguirregabiria, V., Mira, P., 2010. Dynamic discrete choice structural models: A survey. Journal of Econometrics 156, 38–67.

Astier, N., Bouquet, P.-F., Lambin, X., 2023. Riding together: eliciting travelers' preferences for long-distance carpooling. Available at SSRN 4360029.

Baldassare, M., Ryan, S., Katz, C., 1998. Suburban attitudes toward policies aimed at reducing solo driving. Transportation 25, 99–117.

Bucher, D., Mangili, F., Cellina, F., Bonesana, C., Jonietz, D., Raubal, M., 2019. From location tracking to personalized eco-feedback: A framework for geographic information collection, processing and visualization to promote sustainable mobility behaviors. Travel behaviour and society 14, 43–56.

Bueno, P.C., Gomez, J., Peters, J.R., Vassallo, J.M., 2017. Understanding the effects of transit benefits on employees' travel behavior: Evidence from the New York-New Jersey region. Transportation Research Part A: Policy and Practice 99, 1–13.

Chen, S.-Y., 2016. Green helpfulness or fun? Influences of green perceived value on the green

loyalty of users and non-users of public bikes. Transport Policy 47, 149–159.
Cooper, R., John, A., 1988. Coordinating coordination failures in Keynesian models. The Quarterly Journal of Economics 103, 441–463.
Correia, G., Viegas, J.M., 2011. Carpooling and carpool clubs: Clarifying concepts and assessing value enhancement possibilities through a Stated Preference web survey in Lisbon, Portugal. Transportation Research Part A: Policy and Practice 45, 81–90.
De Vos, J., Waygood, E.O.D., Letarte, L., 2020. Modeling the desire for using public transport. Travel Behaviour and Society 19, 90–98.
De Witte, A., Hollevoet, J., Dobruszkes, F., Hubert, M., Macharis, C., 2013. Linking modal choice to motility: A comprehensive review. Transportation Research Part A: Policy and Practice 49, 329–341.
Epstein, J.M., 2012. Generative Social Science: Studies in Agent-Based Computational Modeling: Princeton University Press.
Gaspoz Frédéric , Canalda Philippe. "Problème de Covoiturage Flexible et sa Résolution avec l'Algorithme GbFCA à base gloutonne Gaspoz, 26ème congrès annuel de la société française de recherche opérationnelle et d'aide à la décision (ROADEF) ENPC, Institut Polytechnique de Paris, Marne-la-Vallée, France 26-28 février 2025, 2 pages,
Geels, F.W., 2011. The multi-level perspective on sustainability transitions: Responses to seven criticisms. Environmental innovation and societal transitions 1, 24–40.
Gheorghiu, A., Delhomme, P., 2018. For which types of trips do French drivers carpool? Motivations underlying carpooling for different types of trips. Transportation Research Part A: Policy and Practice 113, 460–475.
Granovetter, M., 1978. Threshold Models of Collective Behavior. American Journal of Sociology 83, 1420–1443.
Hammadou, H., Papaix, C., 2015. Policy packages for modal shift and CO2 reduction in Lille, France. Transportation Research Part D: Transport and Environment 38, 105–116.
Hansen, L.P., 1982. Large sample properties of generalized method of moments estimators. Econometrica: Journal of the econometric society 1029–1054.
Julagasigorn, P., Banomyong, R., Grant, D.B., Varadejsatitwong, P., 2021. What encourages people to carpool? A conceptual framework of carpooling psychological factors and research propositions. Transportation Research Interdisciplinary Perspectives 12, 100493.
Joliot Anna, Philippe Canalda, Hakim Mabed, Gérard Cécé. "Premières Résolutions PLNE du Covoiturage Flexible", 26ème congrès annuel de la société française de recherche opérationnelle et d'aide à la décision (ROADEF) ENPC, Institut Polytechnique de Paris, Marne-la-Vallée, France 26-28 février 2025, 2 pages
Katz, M.L., Shapiro, C., 1985. Network externalities, competition, and compatibility. The American economic review 75, 424–440.
Konishi, H., Mun, S., 2010. Carpooling and congestion pricing: HOV and HOT lanes. Regional Science and Urban Economics 40, 173–186.
Laroche, F., Lamatkhanova, A., 2022. Effects of open access competition on prices and frequencies on the interurban railway market: Evidence from Europe. Research in Transportation Business & Management 43, 100705.
Laroche, F., Schemeleva, K., 2026. Exploratory study of long-distance carpooling supply and public financial incentives: The case of France. Research in Transportation Economics 116, 101734.
Lind, H.B., Nordfjærn, T., Jørgensen, S.H., Rundmo, T., 2015. The value-belief-norm theory, personal norms and sustainable travel mode choice in urban areas. Journal of Environmental Psychology 44, 119–125.
McFadden, D., 1974. The measurement of urban travel demand. Journal of public economics 3, 303–328.

Monchambert, G., 2020a. Why do (or don't) people carpool for long distance trips? A discrete choice experiment in France. Transportation Research Part A: Policy and Practice 132, 911–931.
Monchambert, G., 2020b. Why do (or don't) people carpool for long distance trips? A discrete choice experiment in France. Transportation Research Part A: Policy and Practice 132, 911–931.
Mounmemi, M., Kouandou, A., 2026. Participation in ROSCAs as a Driver of the Household Energy Transition in Cameroon. J of Intl Development jid.70081.
Neoh, J.G., Chipulu, M., Marshall, A., 2017. What encourages people to carpool? An evaluation of factors with meta-analysis. Transportation 44, 423–447.
Newey, W.K., McFadden, D., 1994. Large sample estimation and hypothesis testing. Handbook of econometrics 4, 2111–2245.
Olave-Cruz, I., Stéphan, M., Volle, A., Zhu, D., 2025. Does Carpooling Reduce Carbon Emissions? The Effect of Environmental Policies in France. Environ Resource Econ 88, 1111–1144.
Otto, I.M., Donges, J.F., Cremades, R., Bhowmik, A., Hewitt, R.J., Lucht, W., Rockström, J., Allerberger, F., McCaffrey, M., Doe, S.S.P., Lenferna, A., Morán, N., Van Vuuren, D.P., Schellnhuber, H.J., 2020a. Social tipping dynamics for stabilizing Earth's climate by 2050. Proc. Natl. Acad. Sci. U.S.A. 117, 2354–2365.
Otto, I.M., Donges, J.F., Cremades, R., Bhowmik, A., Hewitt, R.J., Lucht, W., Rockström, J., Allerberger, F., McCaffrey, M., Doe, S.S.P., Lenferna, A., Morán, N., Van Vuuren, D.P., Schellnhuber, H.J., 2020b. Social tipping dynamics for stabilizing Earth's climate by 2050. Proc. Natl. Acad. Sci. U.S.A. 117, 2354–2365.
Pangbourne, K., Mladenović, M.N., Stead, D., Milakis, D., 2020. Questioning mobility as a service: Unanticipated implications for society and governance. Transportation research part A: policy and practice 131, 35–49.
Pavón, N., Rizzi, L.I., 2019. Road infrastructure and public bus transport service provision under different funding schemes: A simulation analysis. Transportation Research Part A: Policy and Practice 125, 89–105.
Piwek, L., Pollick, F., Petrini, K., 2015. Audiovisual integration of emotional signals from others' social interactions. Frontiers in psychology 9, 116.
Rochet, J.-C., Tirole, J., 2003. Platform competition in two-sided markets. Journal of the european economic association 1, 990–1029.
Rotaris, L., Danielis, R., 2014. The impact of transportation demand management policies on commuting to college facilities: A case study at the University of Trieste, Italy. Transportation Research Part A: Policy and Practice 67, 127–140.
Salihou, F. 2023. Economic and non-economic incentives for modal shift toward sustainable mobility solutions (Doctoral dissertation, Université Paris-Saclay).
Salihou, F., Bulteau, J., Le Boennec, R., Berrada, J., Da Costa, P., 2026. The impacts of combining incentives on carpooling for commuting in the Paris region. Journal of Environmental Planning and Management 69, 649–675.
Shaheen, S.A., Cohen, A.P., 2013. Carsharing and Personal Vehicle Services: Worldwide Market Developments and Emerging Trends. International Journal of Sustainable Transportation 7, 5–34
Simon, C.P., Blume, L., 1994. Mathematics for economists. Norton New York.
Standing, C., Standing, S., Biermann, S., 2019. The implications of the sharing economy for transport. Transport Reviews 39, 226–242.
Tafreshian, A., Masoud, N., 2020. Using subsidies to stabilize peer-to-peer ridesharing markets with role assignment. Transportation Research Part C: Emerging Technologies 120, 102770.
Totouom, A., 2024. Women's decision-making power and the adoption of liquefied petroleum

gas for cooking in Cameroon. Energy Policy 184, 113912.
Tsirimpa, A., Polydoropoulou, A., Pagoni, I., Tsouros, I., 2019. A reward-based instrument for promoting multimodality. Transportation research part F: traffic psychology and behaviour 65, 121–140.
Ungemah, D., Goodin, G., Dusza, C., Burris, M., 2007. Examining incentives and preferential treatment of carpools on managed lane facilities. Journal of Public Transportation 10, 151–169.
Wang, Y., Monchambert, G., 2026. Does subsidy increase the use of carpooling via platforms? The case of short-distance carpooling in France. Transportation Research Part A: Policy and Practice 203, 104767.